Theor Chem Acc (2001) 106:194–198
DOI 10.1007/s002140100262

Theoretical
Chemistry Accounts

Regular article

Study of association of 2-methoxyethanol in the aqueous phase

Mohsen Tafazzoli, Safeallah Jalili

Department of Chemistry, Sharif University of Technology, P.O. Box 11365-9516, Tehran, Iran

Received: 9 October 2000 / Accepted: 5 January 2001 / Published online: 3 May 2001

Abstract. Monte Carlo simulations have been carried out for 2-methoxyethanol in an isothermal–isobaric ensemble (NPT) at 298.15 K and 1 atm pressure. The optimized potential for liquid simulation force field parameters has been used for modeling 2-methoxyethanol and the TIP4P model for water. Intramolecular rotations are described by an analytical potential function fitted to ab initio energies. It has been shown that the water molecules can form hydrogen bonds between adjacent O atoms of $CH_3OCH_2CH_2OH$ in aqueous media. The self-association of 2-methoxyethanol in aqueous media has been studied by statistical perturbation theory.

Key words: Monte Carlo simulation – Potential of mean force – Optimized potential for liquid simulation – 2-Methoxyethanol – TIP4P

1 Introduction

Compounds with formula X–CH_2CH_2–Y, where the X and Y groups can be electron donating or electron withdrawing, have been the subject of studies using different techniques in recent years. In the gas phase some of the related conformers are stable owing to intramolecular hydrogen bonds [1], but different behavior was found in the solution phase [2]. Compounds with general formula $C_mH_{2m+1}(OCH_2CH_2)_nOH$ or C_mE_n [3] have interesting molecular and aggregation properties and several commercial and pharmacological applications [4–6]. The unique duality of the C_1E_1 molecule towards an aqueous environment leads to a rich spectrum of complex self-association phenomena, while simple solute molecules and water do not exhibit such phenomena.

The association phenomenon has several applications in chemistry and biochemistry [7–10]. We have used statistical perturbation theory (SPT) to compute the free-energy profiles and the potential of mean force (PMF) for association of C_1E_1 in water by using Monte Carlo (MC) simulations.

2 Computational details

The statistical mechanics calculations were carried out for computing equilibrium structural and thermodynamic features of the aqueous systems via statistical mechanical average and standard procedures, such as metropolis sampling, periodic boundary conditions and the isothermal–isobaric (NPT) ensemble. Metropolis sampling, augmented by preferential sampling [11–14] was used, in which the probability of attempting to move a solvent molecule is made proportional to $1/(r^2+C)$, where r is distance from the midpoint of the C3–C4 bond in C_1E_1 to the water oxygen. The constant C was set at 89 Å^2, which caused the water molecules nearest the solute to be moved further, as far as the most distant water molecules. The attempt to move the solute every 120 configurations further enhanced the solute–solvent statistics. We performed two series of simulations. In the first series each system consisted of 260 water molecules and one C_1E_1 molecule in a cubic box with dimensions of approximately $20 \times 20 \times 20$ Å^3. The temperature and external pressure were fixed at 25 °C and 1 atm. In the second series, each system consisted of 540 water molecules and two C_1E_1 molecules in a box with dimensions of approximately $33.5 \times 22 \times 22$ Å^3, and the other conditions were as before. There is an equilibration phase in each simulation. Equilibration should continue until the values of a set of monitored properties become stable. In this work, the energy of the system, including solvent–solute interactions, was selected as an equilibration criterion. The intermolecular interactions were spherically truncated at a cutoff distance based on the midpoint of the C3–C4 distance in C_1E_1. The solvent–solvent and solvent–solute interactions were truncated at 9.5 and 10 Å, and were quadratically featured to zero via a switching function over 0.5 Å. New configurations were generated by randomly selecting a monomer, translating it in all three Cartesians directions, rotating it randomly about a randomly chosen axis, and performing any torsional motion. The ranges for three types of motions for solute and solvent molecules are given by $\pm\Delta r$, $\pm\Delta\theta$ and $\pm\Delta\phi$, respectively, in Table 1. Volume changes were attempted every 2410 configurations. The range of all motions was chosen to yield an acceptance ratio of about 44% for the new configuration. The intermolecular and intramolecular interactions were described by an optimized potential for liquid simulation

---

Correspondence to: M. Tafazzoli
e-mail: tafazoli@ch.sharif.ac.ir

Table 1. Computational details for Monte Carlo simulations. $\pm\Delta r$, $\pm\Delta\theta$ and $\pm\Delta\phi$ are the ranges of translating, rotating and torsional motions, respectively. $\pm\Delta V$ is the volume change

Series	Number of water molecules	Number of C_1E_1 molecules	$\pm\Delta r$ (Å)[a]	$\pm\Delta\theta$ (deg)[a]	$\pm\Delta\phi$ (deg)	$\pm\Delta V$ (Å^3)	Number of configurations ($\times 10^{-6}$)[b]
First	260	1	0.17 (0.18)	15 (18)	15	580	1.7 (4)
Second	540	2	0.17 (0.18)	15 (18)	15	600	4 (4.7)

[a] The values in *parentheses* are related to water

[b] The first value is for equilibration and the value in *parentheses* is for sampling

Table 2. Optimized potential for liquid simulation parameters for C_1E_1 (CH3OCH2CH2OH) and water

Site	ε (kJ mol^{-1})	σ (Å)	q(e)
C_1E_1			
CH_3	0.847	3.785	0.265
O	0.818	3.0470	−0.580
CH_2	0.478	3.9830	0.290
CH_2	0.748	3.9830	0.290
O	0.467	3.0700	−0.700
H	0.000	0.0000	0.435
H_2O			
O	0.000	3.154	0.155
H	0.520	0.000	0.000
M[a]	−1.040	0.000	0.000

[a] M is a point on the bisector of the HOH angle, 0.15 Å from the oxygen towards the hydrogens

Table 3. Fourier coefficients for the intramolecular rotational potential function Units for V are kilojoules per mole

	Φ_1	Φ_2	Φ_3
V_1 (RHF/6-31G*)	19.823	−5.811	9.091
V_1 (RMP2/6-31G*)	19.513	−5.923	9.109
V_2 (RHF/6-31G*)	3.138	−0.925	12.845
V_2 (RMP2/6-31G*)	3.222	−0.955	12.587
V_3 (RHF/6-31G*)	3.498	−0.711	3.130
V_3 (RMP2/6-31G*)	3.592	−0.722	3.251

(OPLS) force field and a united atom representation was used. The general form of the intermolecular functions includes Coulomb and Lennard-Jones potentials between interaction sites on the two molecules, a and b (Eq. 1) [15, 16].

$$\Delta E = \sum_{i}^{a} \sum_{j}^{b} \left(\frac{q_i q_j e^2}{r_{ij}} + \frac{A_{ij}}{r_{ij}^{12}} - \frac{C_{ij}}{r_{ij}^{6}} \right) \qquad (1)$$

The summation is over the individual interactions between all pairs of atomic sites, j and i, in those molecules. Standard combining rules are used as follows: $A_{ij} = (A_{ii}A_{jj})^{1/2}$ and $C_{ij} = (C_{ii}C_{jj})^{1/2}$. The A and C parameters may also be expressed in terms of Lennard-Jones ε and σ as $A_{ii} = 4\varepsilon_i\sigma_i^{12}$ and $C_{ii} = 4\varepsilon_i\sigma_i^{6}$. For C_1E_1 the CH_2 and CH_3 groups on the chain atoms were modeled as united atoms (sites) and the oxygen and terminating hydrogen as discrete atoms. The C_1E_1 were modeled using OPLS molecular force field parameters [13, 17] and all OPLS parameters for this molecule are summarized in Table 2. The four-site TIP4P model [16] for water was used in this context, in conjunction with the OPLS potential (Table 2).

Torsional motion about C2–C3, C3–C4 and C4–O5 bonds was included in the simulation. The torsional parameters for all dihedrals and Lennard–Jones parameters due to 1,5 nonbonded interactions in C_1E_1 were obtained by using ab initio calculations (RHF/6-31G* level). The Fourier series describes the rotational potential energy [14]:

Table 4. Calculated Lennard-Jones parameters for 1,5 nonbonded interactions

1,5 nonbonded interaction parameters	ε (kJ mol^{-1})	σ (Å)
C1–O5 (RHF/6-31G*)	0.00669	3.366
C1–O5 (RMP2/6-31G*)	0.007	3.565
C2–H6 (RRHF/6-31G*)	0.02970	2.800
C2–H6 (RMP2/6-31G*)	0.03012	2.720

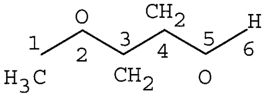

$$\phi_1 = C1O2 - C3C4$$

$$\phi_2 = O2C3 - C4O5$$

$$\phi_3 = C3C4 - O5H6$$

Fig. 1. Numbering of the atoms and dihedral angles of 2-methoxyethanol

$$V(\phi) = V_1/2[1 + \cos(\phi)] + V_2/2[1 - \cos(2\phi)] + V_3/2[1 + \cos(3\phi)] \quad . \qquad (2)$$

There is one equation for each of the three dihedral angles of C_1E_1, and it is similar to Eq. (2). For such molecules the Fourier series need to be augmented by a 1,5 Lennard-Jones potential as follows:

$$V(\phi, r) = \sum_{i=1}^{3} V(\phi_i) + \sum_{i<j}^{>1,4} \left(A_{ij}/r_{ij}^{12} - C_{ij}/r_{ij}^{6} \right) \quad . \qquad (3)$$

The Fourier coefficients and the Lennard-Jones parameters were coupled in the fitting by nonlinear least-squares regression. In general, the use of RHF/6-31G* or a higher level of ab initio quantum mechanical calculations is a well-accepted procedure for calculation of torsional parameters [18–20]. In this work we use this procedure for obtaining the coefficients in the Fourier series: V_1, V_2 and V_3. For this purpose an energy scan was performed for examples of the missing torsions with RHF/6-31G* calculations. A full geometry optimization was done at each point with the exception of the chosen dihedral angle. For testing the reliability of the method, the calculation was carried out using RMP2/6-31G*. The parameters calculated for the Fourier series are shown in Table 3 and the Lennard-Jones parameters for 1,5 interactions for C_1E_1 are shown in Table 4. The comparison of the results for the Fourier coefficients and the Lennard-Jones parameters for 1,5 interactions predicted by different methods shows good agreement between them.

The presence of hydrogen bonding was monitored for coordinates saved every 4×10^4 configurations during the simulation.

The PMF for association of C_1E_1 in aqueous media was determined by using SPT [21]. Briefly, one of the possibilities of calculating the Gibbs free energy of association is based on SPT, from which

$$\Delta G_{\mathrm{BA}} = -k_{\mathrm{B}}T \ln\langle \exp(-\beta \Delta E_{\mathrm{BA}}) \rangle_{\mathrm{A}} \ , \tag{4}$$

where k_{B} is the Boltzmann constant, T the absolute temperature and $\beta = (k_{\mathrm{B}}T)^{-1}$. ΔE_{BA} denotes the difference in energy between the two systems A and B at a given configuration, and $\langle \cdots \rangle_{\mathrm{A}}$ denotes the ensemble average corresponding to system A. In MC simulations, the ensemble average is approximated by a set of sampled configurations. Since sampling is performed for system A, it must be ensured that the set of configurations generated includes a set of configurations representing state B. If states A and B do not overlap in phase space, then the values of the calculated free-energy differences will not be very accurate, because we have not adequately sampled the phase space of B when simulating A. If the two states A and B differ strongly, ΔE_{BA} will generally be very large,

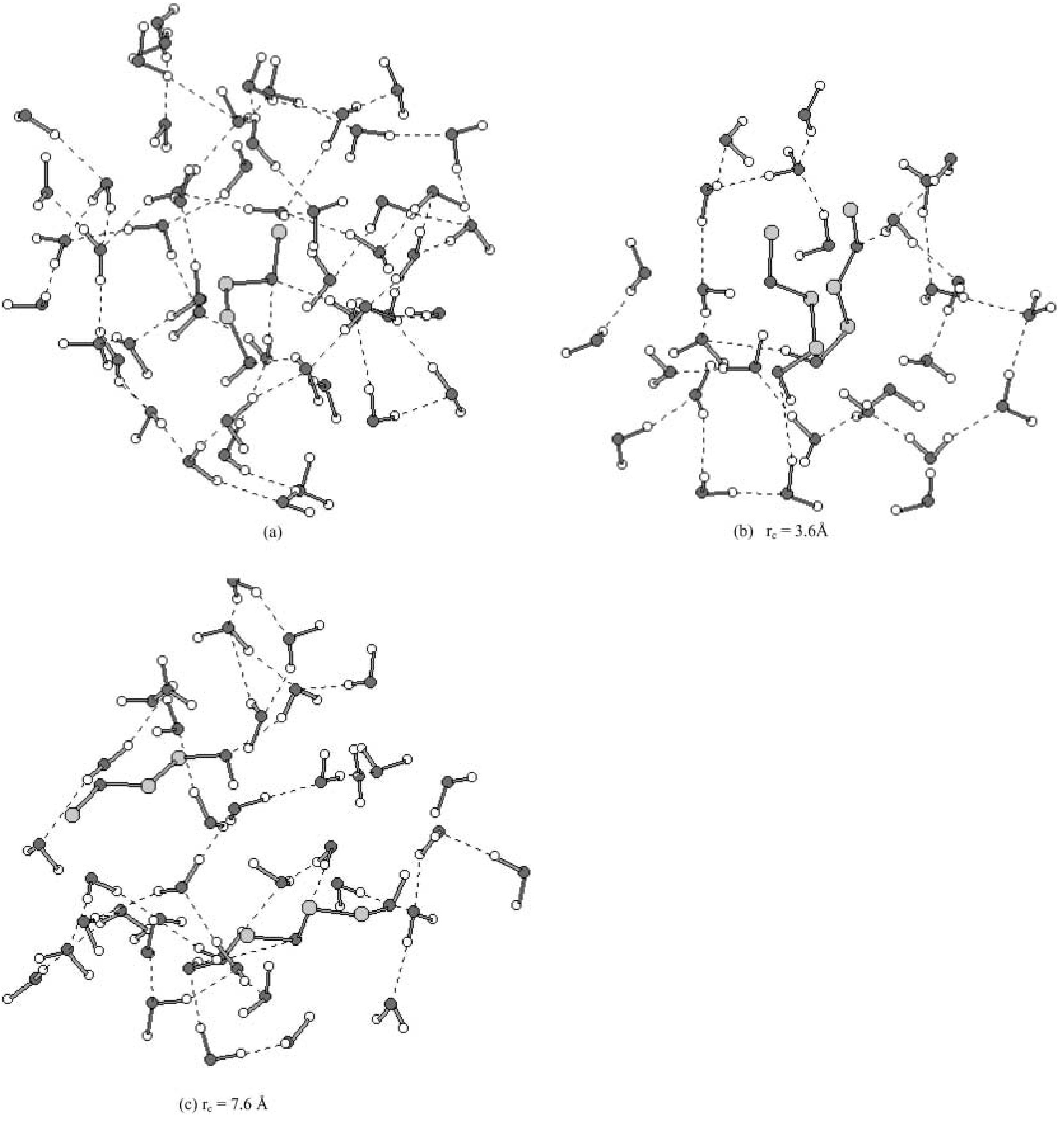

Fig. 2a–c. Equilibrium configuration of the interaction between 2-methoxyethanol molecules and solvent molecules in aqueous media. **a** One solute molecule in a solvent box. **b** Two solute molecules in a solvent box, contact structure. **c** Two solute molecules in a solvent box, solvent-separated structure. (*Open*, *dark* and *gray circles* are hydrogen, oxygen and carbon atoms, respectively)

and the simulation period needed to converge Eq. (4) will exceed the feasible computational period. In this case, the perturbation may be split into n smaller increments, so-called windows; for each of these, the free-energy differences can be determined individually as follows [22, 23]:

$$\Delta G_{\mathrm{BA}} = \sum_{i=0}^{n-1} \Delta G_{i\rightarrow i+1} \ , \tag{5}$$

in which

$$\Delta G_{1\rightarrow i+1} = -k_{\mathrm{B}}T \ln\langle \exp(-\beta\Delta E_i)\rangle_i \ , \tag{6}$$

where n is the number of windows and $\Delta E_i = E_{i+1}-E_i$. Sampling at an intermediate system i enables us to calculate the free-energy differences to the $i+1$ and $i-1$ systems. Hence, one simulation allows the simultaneous calculation of two free-energy differences. This technique is called "double-wide" sampling [24, 25]. The total free energy is the average of the forward and backward free energies obtained during the simulation.

In this work the reaction coordinate (r_c) was chosen between the midpoints of the C3–C4 bond distances in two C_1E_1, and the SPT was used by sequentially perturbing along the r_c in steps of 0.2 Å (each center moved in or out by 0.1 Å). For each r_c a full simulation was carried out.

All MC simulations were executed with a personal computer, by using a program which was written by our group in C+ + language and which was designed for MC simulation of the liquid phase [26, 27]. All ab initio calculations at the HF/6-31G* and MP2/6-31G* leves were carried out with GUASSIAN 92 package [28], adapted for a personal computer.

3 Results and discussion

The numbering of the atoms in C_1E_1 is shown in Fig. 1. Rigid bond lengths and angles were used in the MC simulation. According to our first series of MC simulations, the most stable conformer in solution is that where the water molecules form hydrogen bonds between two oxygen atoms in the C_1E_1 molecule; in other words, water molecules have a strong tendency to form hydrogen-bonding bridges between two oxygen atoms on the same chain (Fig. 2). In the views shown in Fig. 2 only the nearest-neighbor water is shown. We think that the effect of this phenomenon is to favor gauche conformations for the central torsional bond.

The formation of hydrogen bonds can be indicated by either geometrical criteria or energy criteria, when the N · · · H or O · · · H distance in the molecules is less than 2.5 Å and/or the interaction energy of molecules is not more positive than -9.418 kJ mol^{-1}, respectively [29]. Hydrogen-bonding analysis was performed for coordinates saved every 4×10^4 configurations during the simulations. We predicted that the average number of hydrogen bonds between solute and solvent is 1.73 and that the average energy is -24.52 kJmol^{-1}. For studying the aggregation phenomena of C_1E_1 a distinct series of simulations was carried out. We performed 15 complete simulations to span the r_c range from 3 to 8.2 Å and the relative free energies were obtained. The relative free energy is shown against reaction r_c in Fig. 3. There are two minima in this curve, corresponding to contact and solvent separated pairs, which occur at 5.1 and 7.8 Å, respectively. This trend is the same as the one found in hydrophobic molecules [30–34]. As shown in Fig. 3 the second minimum appears at higher energy compared with the first one, and this indicates the importance of contact pairs. Therefore in spite of the presence of OH and CH_3O groups, the C_1E_1 molecule behaves like a hydrophobic molecule. The depth of the minima in Fig. 3 indicates almost strong aggregation. At a short r_c the number of hydrogen bonds decrease owing to the association of solute molecules. Considering Fig. 2 there is no internal hydrogen bond in the C_1E_1 molecule, and the most hydrogen bonds are between C_1E_1 and water molecules; thus, the formation of a hydrogen bond between water molecules and C_1E_1 molecules is more feasible than the formation of a hydrogen bond between C_1E_1 molecules. Regarding these results it can be said that the hydrophilic groups do not affect the aggregation phenomena. It is possible that water molecules hinder the rotational motion of C_1E_1, which is supported by the small change in the related conformation during the simulations. The computed intramolecular energy around the OC–CO bond in the gas and liquid phases is shown in Fig. 4. $S(\phi)$ is full dihedral angle distribution. The $S(\phi)$ values for an ideal gas are derived from the Boltzmann distribution for $V(\phi)$. The difference between the curves of the two phases is due to intermolecular hydrogen bonding in the liquid phase and to intramolecular hydrogen bonding in the gas phase [4]. In some of the r_c (e.g. 5.4 and 6.2 Å), water molecules form hydrogen-bond bridges (not regular bridges) between two solute molecules; this does not happen at large r_c. The presence of the CH_3O– group in the molecules affects these bridges owing to the weak tendency for the formation of intermolecular hydrogen bonds in solution in comparison to the gas phase. Inspection of the views reveals that hydrogen-bond formation is mainly between the C_1E_1 and solvent molecules.

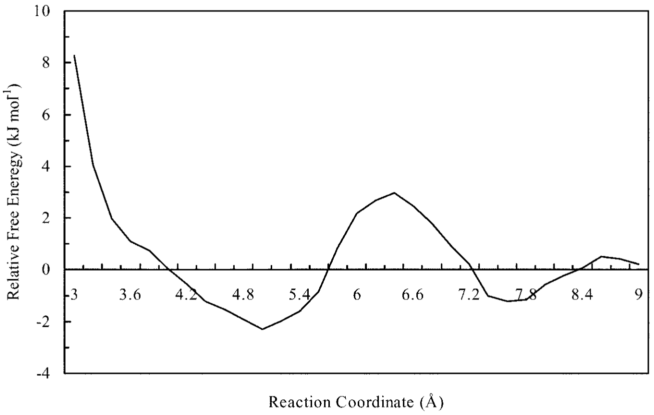

Fig. 3. Relative free energy for self-association of 2-methoxyethanol in water

4 Conclusion

2-Methoxyethanol has been found to form internal hydrogen bonds in the gas phase [1], while in solution the water molecules form hydrogen bonds between adjacent O atoms in 2-methoxyethanol. In the condensed phase the populations differ from the gas phase, which was found through MC simulations. The

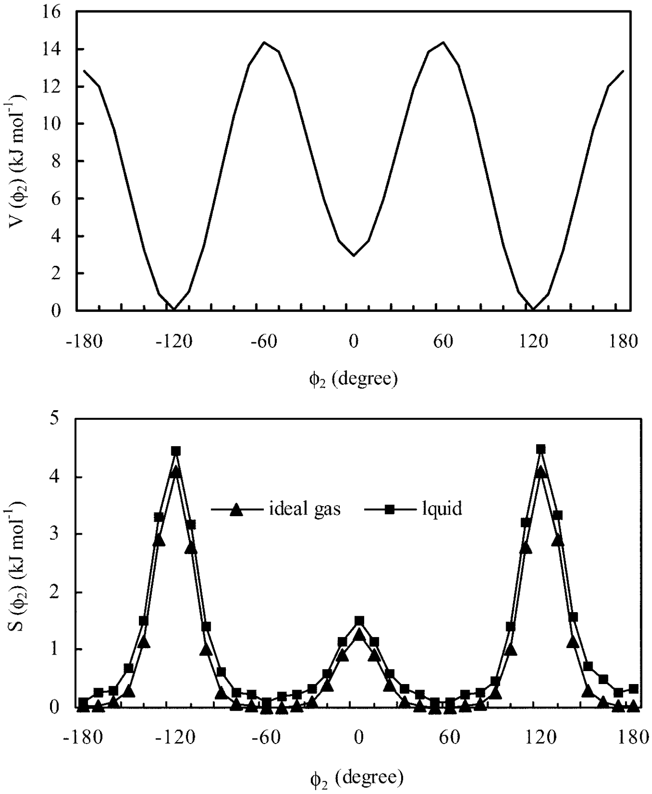

Fig. 4. (*Top*) Potential function for rotation around the C3–C4 bond in 2-methoxyethanol. (*Bottom*) Dihedral angel distribution in 2-methoxyethanol. The units for $V(\phi)$ are kilocalories per mole and for $S(\phi)$ are mole percent per degree

free-energy profiles for 2-methoxyethanol showed two minima (at $r_c = 5.1$ and 7.7 Å) corresponding to contact and solvent-separated pairs. The tendency to form hydrogen-bond bridges is larger than the tendency to form internal hydrogen bonds for larger r_c values. In this case, water molecules between two solutes formed bridges. This shows that the formation of such bridges could be an effective driving force for the association of hydrophilic groups.

References

1. Gil FPS, Fausto R, Amorim da Costa AM, Teixeira-Dias JJC (1994) J Chem Soc Faraday Trans 90: 689
2. Price DJ, Roberts JD, Jorgensen WL (1998) J Am Chem Soc 120: 9672
3. Van Os NM, Aaak JR, Rupert LAM (1993) Physico-chemical properties of selected anionic, cationic and nonionic surfactants. Elsevier, Amsterdam, pp 289
4. Price DJ, Roberts JD, Jorgensen WL (1998) J Am Chem Soc 120: 9672
5. (a) Kong YC, Nicholson D, Parsonage NG (1994) J Chem Soc Faraday Trans 90: 2375; (b) Kong YC, Nicholson D, Parsonage NG (1995) J Chem Soc Faraday Trans 91: 4261
6. Myers D (1998) Surfactant science and technology. Chapman & Hall, New York
7. Durell ST, Brooks BR, Ben-Naim A (1994) J Phys Chem 98: 2198
8. Mezei M, Ben-Naim A (1990) J Chem Phys 92: 1359
9. Ben-Naim A (1990) Biopolymers 29: 567
10. Ben-Naim A (1990) J Chem Phys 93: 8196
11. Jorgensen WL, Madura JD, Swensen CJ (1984) J Am Chem Soc 106: 6638
12. Jorgensen WL, Swensen CJ (1985) J Am Chem Soc 17: 569
13. Jorgensen WL (1986) J Phys Chem 90: 1276
14. Jorgensen WL, Swensen CJ (1985) J Am Chem Soc 107: 1489
15. Jorgensen WL, Tirado-Rives J (1988) J Am Chem Soc 110: 1657
16. Jorgensen WL, Chandraskhor J, Madura RW, Klein ML (1983) J Chem Phys 79: 926
17. Jorgensen WL (1981) J Am Chem Soc 103: 335
18. Rizzo RC, Jorgensen WL (1999) J Am Chem Soc 121: 4827
19. Jorgensen WL, Maxwell DS, Tirado-Rives J (1996) J Am Chem Soc 118: 11225
20. Damm W, Frontera A, Tirado-Rives J, Jorgensen WL (1997) J Comput Chem 16: 1955
21. Zwanzig R (1954) J Chem Phys 22: 1420
22. Leach AR (1996) Molecular modeling: principles and applications. Wesley Longman, pp 408
23. Jorgensen WL, Blake JF, Buckner JK (1989) Chem Phys 129: 193
24. Jorgensen WL, Ravimohom CJ (1985) J Chem Phys 83: 3050
25. Jorgensen WL (1983) J Phys Chem 87: 5304
26. Tafazzoli M, Jalili S (2000) Chem Phys Lett 331: 242
27. Tafazzoli M, Jalili S (2000) J Mol Liq 89: 31
28. Foresman JB, Johnson BG, Schlegel HB, Robb MA, Replogle ES, Romperts R, Andres JL, Raghavachari K, Binkley JS, Gonzalez C, Martin RL, Fox DJ, Defrees DJ, Baker J, Stewart JJP, Pople JA (1992) Gaussian 92, revision D.2. Gaussian, Pittsburgh, Pa
29. Duffy EM, Kowalczyk PJ, Jorgensen WL (1993) J Am Chem Soc 115: 271
30. Jorgensen WL, Buckner JK, Boudon S, Tirado-Rives J (1988) J Chem Phys 89: 3742
31. Smith DE, Zhang L, Haymet DJ (1992) J Am Chem Soc 114: 5875
32. Smith DE, Haymet DJ (1993) J Chem Phys 98: 6445
33. Jungwirth P, Zahradník R (1994) Chem Phys Lett 101: 5116
34. Lüdeman S, Abseher R, Schreiber H, Steinhauser O (1997) J Am Chem Soc 119: 4206